ELSEVIER

Cement & Concrete Composites 24 (2002) 437–449

Cement & Concrete Composites

www.elsevier.com/locate/cemconcomp

Monitoring electrical resistance of concretes containing alternative cementitious materials to assess their resistance to chloride penetration

P.A.M. Basheer [a,*], P.R.V. Gilleece [a], A.E. Long [a], W.J. Mc Carter [b]

[a] *Faculty of Engineering, School of Civil Engineering, The Queen's University of Belfast, Stranmillis Road, Belfast, Northern Ireland BT7 1NN, UK*
[b] *Department of Civil and Offshore Engineering, Heriot-Watt University, Edinburgh EH14 4AS, UK*

Abstract

Chloride ion penetration into concrete and the resulting deterioration (cracking and spalling due to the corrosion of reinforcement) is a major concern of engineers and owners of bridges and marine structures. Several publications have reported the excellent performance of concrete containing alternative cementitious materials (ACMs), such as pulverised fuel ash (PFA), ground granulated blast furnace slag (GGBS), microsilica (MS) and metakaolin (MK) in marine environment and highway structures. The resistance offered by these concretes has been related to the low mobility of chloride ions due to either the reduction in the number of interconnected pores as a result of the pozzolanic reaction of the ACMs or the chemical binding with the cement hydrates. However, the secondary reaction products are formed slowly in Portland cement concrete containing ACMs and as a result it is likely that the resistance offered to the penetration of chloride ions also increases slowly with time. In order to monitor the continuous behaviour of concretes containing these ACMs in a chloride exposure regime, an investigation was carried out, the results of which are reported in this paper. Ten different concrete mixes were subjected to a cyclic ponding regime with 0.55 M sodium chloride solution and the changes in concrete were monitored by measuring the changes in resistance between pairs of stainless steel electrodes embedded in the concrete at different depths from the exposed surface. The test was continued for nearly one year. The results indicated that, although the resistance of concrete decreased initially due to the penetration of chlorides, in the longer term the resistance of concretes containing ACMs outperformed the control concrete made with ordinary Portland cement (OPC). Drilled dust samples extracted after different durations of ponding were tested for the chloride content, which confirmed that the increase in resistance of the ACMs was due to the combined effects of the reduction in the penetration of chlorides and the continuous hydration activity of the ACMs.

Keywords: Pulverised fuel ash; Ground granulated blast furnace slag; Microsilica; Metakaolin; Electrical resistivity; Chloride ingress; Alternative cementitious materials

1. Introduction

Deterioration of concrete due to corrosion of reinforcement is the most serious durability problem faced by the construction industry [1]. The corrosion of steel in concrete normally occurs as a result of either the reduction in alkalinity at the steel, due to carbonation of concrete or leaching of alkalis, or the presence of a significant quantity of chloride ions in the concrete. Soluble chlorides in deicing salts or those occurring naturally in soils, seawater and groundwater can penetrate the concrete cover by absorption through its surface, diffusion in interconnected capillary pores or by direct access through cracks in the concrete. Although the primary mechanism of chloride transport for the near-surface unsaturated concrete is absorption, the accumulation of chlorides in this layer leads to further penetration of chlorides into concrete by diffusion [2]. As a consequence, diffusion becomes the most dominant mechanism of chloride transport at greater depths. It is in this context that the beneficial effects of alternative cementitious materials (ACMs) should be considered.

When ACMs, such as pulverised fuel ash (PFA) and ground granulated blast furnace slag (GGBS), are used

* Corresponding author. Tel.: +44-028-9027-4006; fax: +44-028-9066-3754.
E-mail address: m.basheer@qub.ac.uk (P.A.M. Basheer).

0958-9465/02/$ - see front matter
PII: S0958-9465(01)00075-0

in concrete, not only the porosity is reduced but also the pores become finer and the change in mineralogy of the cement hydrates leads to a reduction in the mobility of chloride ions [3]. The initial protection against chloride penetration provided by concretes containing the ACMs may depend on the type of the material, the duration of curing and the age of concrete when it is exposed to the chloride environment. For instance, the hydration of both PFA and GGBS requires sufficient quantities of calcium hydroxide to be released due to the hydration of the Portland cement [4]. On the other hand, both microsilica (MS) and metakaolin (MK) react with calcium hydroxide released by the hydration of Portland cement at a faster rate than PFA and GGBS, so that they perform better even at early ages. When the long-term protection against chloride penetration is dealt with, both the type of ACM and the exposure regime may have a significant influence. It is in these contexts that the current investigation was carried out with the primary objective of assessing the long-term performance of concretes containing PFA, GGBS, MS and MK in a wetting and drying chloride exposure regime.

2. Experimental programme

2.1. Layout of the test programme and preparation of test specimens

The investigation was carried out on 10 concrete mixes containing Portland cement, PFA, GGBS, MS and MK (Table 1). A mix ratio of 1:1.65:3 by mass was used between the cementitious materials, fine aggregate and coarse aggregate, with a water–cementitious materials ratio of 0.52. While including the ACMs in the mixes, the proportioning was done by mass and any change in water demand due to them was not accounted for in the total water used in the mixes. The mix ratio (i.e., the proportions of both the fine and the coarse aggregates) was slightly altered while adding the 5% MS and 5% MK to both the PFA and GGBS mixes. As the intention was to monitor the long-term protection of various mixes, the effect of these variations is not considered to be relevant for this paper. Table 2 presents the chemical composition and Table 3 reports the physical properties of the cementitious materials used in this investigation. The fine aggregate was medium graded sand [5] and the coarse aggregate was 10 mm crushed basalt. Table 4 presents the physical properties of the aggregates used.

Table 1
Composition of mixes

Mix	Composition	Notation
1	100% OPC	OPC
2	70% OPC + 30% PFA	PFA30
3	70% OPC + 30% PFA + 5% MS	PFA-MS5
4	70% OPC + 30% PFA + 5% MK	PFA-MK5
5	50% OPC + 50% GGBS	GGBS50
6	50% OPC + 50% GGBS + 5% MS	GGBS-MS5
7	50% OPC + 50% GGBS + 5% MK	GGBS-MK5
8	90% OPC + 10% MS	MS10
9	90% OPC + 10% MK	MK10
10	80% OPC + 20% MK	MK20

Table 2
Chemical composition of the cementitious materials

Property	OPC	PFA	GGBS	MS	MK
SiO_2	21.8	48.9	35.0	93.2	54.8
Al_2O_3	4.2	29.1	11.0	0.1	41.2
Fe_2O_3	2.5	10.9	1.0	0.3	0.57
CaO	65.1	2.0	41.0	1.0	0.02
MgO		1.4	8.0	0.2	0.31
Na_2O	0.13	0.9		1.82	0.04
K_2O	0.72	3.6			2.27
TiO_2		1.0			0.01
SO_3	2.4	0.72	0.1	0.1	
S			0.9		
Loss on ignition		0.42		1.8	0.8

The ACMs were mixed along with the ordinary Portland cement (OPC) in a dry state prior to the addition to the mix, thus ensuring complete blending between the two. Prior to mixing, the aggregates were oven dried and a pre-determined quantity of water was added to the mix water in order to allow for the absorption of aggregates during the first 1 h after mixing. The concrete was manufactured by following the procedure given in BS 1881: Part 125: 1986 [6]. The fresh concrete was tested for slump and compacting factor, in accordance with BS 1881: Parts 102 [7] and 103 [8], respectively (see Table 5 for the results). Following these tests, the test specimens were manufactured.

The test specimens were 100 mm cubes and $250 \times 250 \times 100$ mm^3 slabs. Fig. 1 gives details of the slabs, which had a dyke cast to retain the 0.55 M sodium chloride solution, four sets of electrodes at an interval of 10 mm from the surface of ponding and a grid at 10 mm intervals from the surface. The electrodes were made of 1.6 mm diameter stainless steel rods and were sleeved from both ends except for a length of 190 mm at the centre. The electrodes projected outside the slab on one side by 50 mm. These were used to monitor the change in resistance of concrete at different depths from the ponded surface with time during the ponding test. The grid on one side of the slab was used to drill dust samples for chloride analysis, again at different depths from the test surface during the ponding test.

Both the slabs and the cubes were manufactured by filling the mould in two layers and vibrating each layer

Table 3
Physical properties of the cementitious materials

Property	OPC	PFA	GGBS	MS	MK
45 μm sieve residue		8.4	0		
Specific gravity	3.18	2.10	2.9	2.1	2.52
Specific surface area (m^2/kg)	200–500	200–600	440	15 000–20 000	14 800

Table 4
Properties of the aggregates

Aggregate type	1 h absorption (%)	Specific gravity	Fineness modulus
Fine aggregate (sand)	1	2.42	1.95
10 mm crushed basalt	0.5	2.73	5.88

Table 5
Slump, compacting factor and 28-day compressive strength of concrete

Mix	Slump		Compacting factor	Compressive strength (MPa)
	Measured (mm)	Slump class[a]		
OPC	48	30–60	0.91	45.46
PFA30	148	60–180	0.96	40.12
PFA-MS5	84	60–180	0.95	31.55
PFA-MK5	94	60–180	0.94	29.32
GGBS50	90	60–180	0.96	40.12
GGBS-MS5	65	60–180	0.94	45.15
GGBS-MK5	67	60–180	0.94	41.00
MS10	19	10–30	0.86	33.45
MK10	27	10–30	0.85	35.06
MK20	9	0–10	0.79	41.5

[a] In accordance with [18].

with a table vibrator. After casting the test specimens, they were left in the mould for 24 h, during which the specimens were covered with a polythene sheet to prevent the evaporation of water from the concrete surface. The specimens were removed from the moulds after 24 h and cured in a water bath at 20(±1) °C for 14 days. They were then placed in a drying cabinet for another 14 days, at a temperature of 40(±1) °C and a relative humidity of 20(±2)%. This was to remove the surface moisture from the slabs and thereby encourage the transport of chlorides by absorption when exposed to the salt solution. After the drying, the slabs were stored in a constant temperature lab, at a temperature of 20(±1) °C and a relative humidity of 55(±1)% for one day.

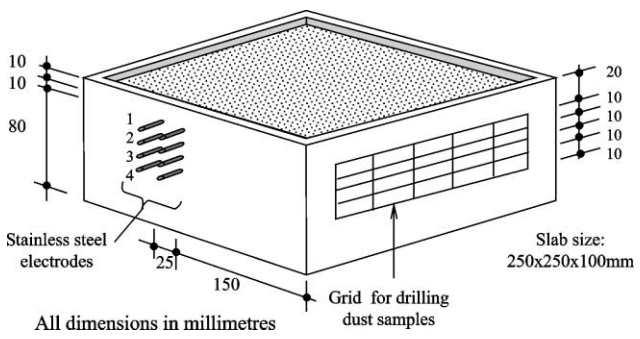

Fig. 1. Concrete slabs used for cyclic ponding test.

Prior to testing, two coats of an epoxy emulsion were applied to the sides of the slabs in order to prevent any absorption of chloride solution through the sides of the slabs in case of a spillage. During the time when the epoxy was being cured, the cubes were tested for the compressive strength, and the results are reported in Table 5.

2.2. Test procedures

At the age of 30 days the slabs were transferred to a constant temperature and humidity room (temperature = 20 ± 1 °C and RH = 55 ± 1%). Prior to the ponding, the conductance between the embedded

electrodes was measured, using the procedure described. Subsequently this measurement was carried out on a weekly basis after ponding.

2.2.1. Chloride ponding regime

A 0.55 M sodium chloride solution was used to pond the slabs for 24 h, on a weekly cycle for one year. A fresh solution of 200 ml was used for each slab during each ponding cycle, in order to ensure that the chloride ion concentration was the same for each week. The effect of evaporation of the solution, if any, was considered to be negligible over the 24-h period. After ponding, the chloride solution was removed from the slabs by using a syringe and any left over solution was mopped off using a sponge. The slabs were then allowed to dry out for the rest of the week, at a temperature of 20(±1) °C and a relative humidity of 55(±1)%.

2.2.2. Measurement of conductance between embedded electrodes

Electrical conduction through concrete is considered to be electrolytic in nature occurring via the continuous, water-filled capillary pores (including microcracks) within the cement matrix [9]. Changes in the resistivity of Portland cement have been found to be minimal after about 10–14 days [10]; after this time, the measured resistance will be dependent upon both the degree of saturation of the capillary pore network and ionic concentrations within the pore water. If there are no external factors influencing the ionic concentrations within the pore water, and if the concrete is completely saturated, a relatively constant resistivity value will be attained after around 14 days [11–15]. However, if there is a change in the degree of saturation, the resistance ratio, R_d/R_s, where R_d is the resistance after the change in degree of saturation and R_s is the resistance of the saturated concrete, can be used to determine this change [9]. Similarly, the change in ionic concentration of a saturated concrete due to the penetration of ions from outside can be obtained by determining the resistance ratio, R_c/R_i [2], where R_c is the resistance of the concrete containing chlorides and R_i is the resistance of the concrete before the exposure. While this is the case for a pore structure which does not change with time, the resistance of concrete could change as a result of continued hydration when ACMs are used in concrete. These changes can be obtained by determining the resistance ratio, R_t/R_o, where R_o represents the resistance between the pair of electrodes prior to the exposure and R_t is the resistance measured with time. This means that the changes in the internal microstructure and the ionic concentration at different depths from an exposure surface can be determined via the resistance ratio. By measuring the conductance of the concrete and inverting the value the resistance can be determined.

The conductance measurements were carried out across consecutive pairs of electrodes in the vertical direction using a conductivity meter with temperature compensation. The conductance readings were inverted to determine the corresponding resistance values and then the resistance ratio, R_t/R_o was determined for each type of concrete. A plot of the resistance ratio with time was then obtained for each concrete mix and these plots were used to compare the performance of different concrete mixes. (*Note*: Ideally these measurements should have been carried out across horizontal pairs of electrodes, kept at 10 mm or less spacing. Nevertheless, it was possible to obtain the variation in internal changes for the different types of cementitious materials used by carrying out measurements between pairs of electrode kept in the vertical direction.)

2.2.3. Chloride profiles

Dust samples were drilled out from five different depths (Fig. 1) after the samples were subjected to 1 week, 1 month, 6 months and 12 months of the cyclic ponding regime. The samples were collected from 5 to 50 mm deep holes drilled parallel to the exposure surface and they were analysed for the chloride ion content. These values were then plotted against the corresponding depths from the surface of ponding to determine the chloride profiles. Immediately after drilling, the holes were filled with cement grout in order to prevent the preferential transport of chlorides along these holes in subsequent ponding cycles.

3. Results and discussion

From the slump, compacting factor and compressive strength values reported in Table 5, it is obvious that the replacement of OPC with both PFA and GGBS results in an increase in workability and a decrease in strength. When the mixes containing PFA and GGBS were supplemented with 5% of both MS and MK by mass, the workability was found to decrease. For the PFA mixes, this decrease in workability was not followed by an increase in strength; however, the strength increased for the GGBS mixes. The performance of the PFA mixes in this investigation was not similar to those reported in publications, presumably because the PFA used was not classified. When both MS and MK were added to the OPC mix, there was a decrease in workability, because these mixes did not include a superplasticiser. As a consequence, the strength was found to decrease. As stated earlier, the primary objective of the investigation was to determine the long-term protection of concrete mixes containing alternative cementing materials against chloride penetration. Therefore, the performance of the mixes will be given emphasis in the following sections.

3.1. Chloride profiles

Figs. 2–4 report the chloride profiles at the end of one year of the cyclic ponding. In these figures the chloride contents are reported in milligram per gram of concrete, expressed as a percentage, rather than converting the values to an equivalent percentage by weight of the cementitious materials. This is because the cement content was not determined while calculating the chloride content from the dust samples. Fig. 2 compares different binary blends with OPC and the effects of adding both MS and MK to the PFA and GGBS concretes are presented in Figs. 3 and 4, respectively.

In Fig. 2, there is a large variation in chloride content between different types of concrete at a depth of 10 mm from the ponded surface. However, beyond 30 mm depth, all binary blends performed equally well compared to the OPC. The lowest chloride content at 10 mm depth was obtained for MK20, which was followed by GGBS50. For both these concretes, the chloride content decreased rapidly to 20 mm depth and only a small amount of chlorides penetrated beyond 30 mm depth.

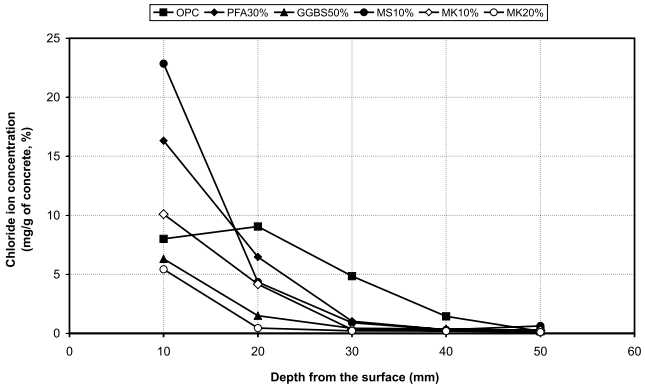

Fig. 2. Chloride profile of concretes made with binary blends after 1 year of exposure.

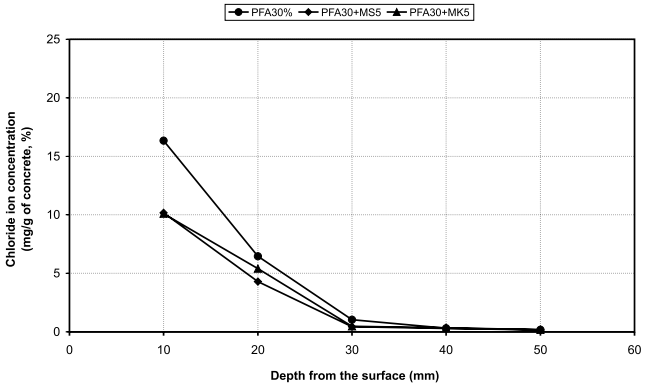

Fig. 3. Chloride profile of PFA concretes made with ternary blends after 1 year of exposure.

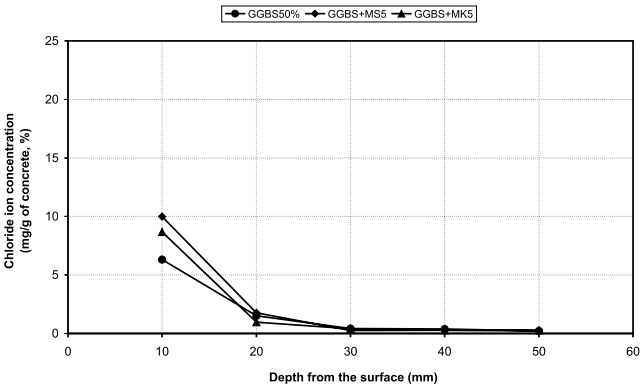

Fig. 4. Chloride profile of GGBS concrete made with ternary blends after 1 year of exposure.

Both the PFA30 and the MS10 concretes had relatively high values of chlorides at 10 mm depth. However, they too had relatively small amount of chlorides beyond 30 mm depth. The chloride content of the MK10 concrete was relatively high at 10 mm depth, however, this was smaller than the value obtained for both the PFA and the MS10 concretes. The performance of this concrete was very similar to that of MK20 beyond 30 mm depth. In the case of the OPC, the chloride content at 10 mm depth was lower than that at 20 mm depth. This is presumably due to carbonation, which is known to push chlorides inward, while modifying the near surface concrete. There was significant penetration of chlorides beyond 30 mm depth for the OPC concrete.

In Fig. 3, both MS and MK resulted in the chloride content at 10 mm depth to decrease by more than 30% for the PFA concrete. However, in Fig. 4 they resulted in a slight increase in the chloride content at this depth for the GGBS concrete. In both cases, there was no effect due to the addition of both MS and MK beyond 20 mm depth. However, it can be noted that the GGBS concretes, both binary and ternary blends, provided better resistance to chloride penetration than the corresponding PFA counterparts.

The chloride profiles in Figs. 2–4 were used to calculate the apparent chloride ion diffusion coefficients for the different types of concrete, by following a procedure outlined by Poulsen [16]. These values are presented in Fig. 5. The best performance was obtained for GGBS50, MK10, MK20, and the two ternary blends with GGBS. This was followed by the three PFA mixes, where the ternary blends performed better than the binary blend. The poorest performance was observed for MS10 and OPC mixes.

The above results indicate that the chloride penetration into the near surface of the MS concrete was similar to that of the OPC concrete. However, when MS is used in concrete, the normal practice is to add a superplasticiser in order to make the concrete more

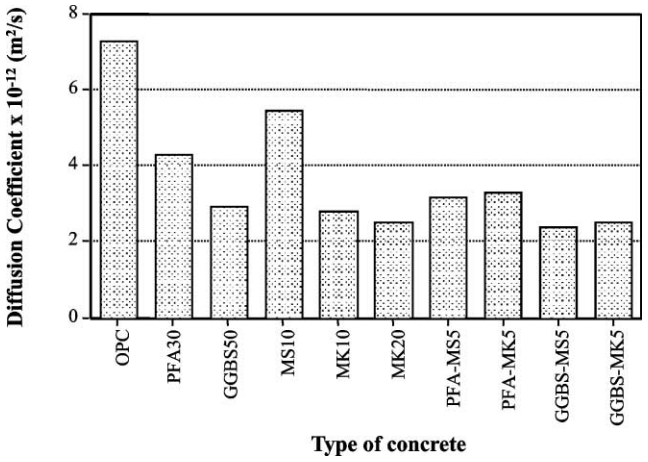

Fig. 5. Apparent diffusion coefficients.

workable. The effect of the improved workability on the chloride penetration was not investigated in the experimental programme.

The addition of MS and MK to unclassified PFA was found to have beneficial effect in reducing the chloride penetration into the PFA concrete. Both GGBS and MK could be used in binary blend form with OPC in order to reduce the chloride penetration. There was no real advantage in adding MS or MK to the GGBS concrete from the point of view of the chloride penetration.

When the chloride penetration and the diffusion coefficients of the different types of concretes are compared with the compressive strength in Table 5, it becomes obvious that the best overall performance was obtained with GGBS50 and MK20. However, the results should be viewed with caution because the workability of the MK20 concrete was poor. If the workability of the mixes was also taken into account (in other words, if the change in water demand was considered while determining the water–cement ratio for a specified workability), then both PFA30 and GGBS50 would probably emerge as the best mixes.

3.2. Resistance variation of the concretes due to chloride ponding

The resistance ratios were calculated by dividing the measured resistances with that of the OPC concrete at 10–20 mm depth when the concrete was dry, i.e., just prior to the start of the ponding cycle. This means that in order to develop the resistance ratio plots, R_t was the as measured resistance values for each type of concrete and R_o was taken to be the resistance of the OPC concrete at 10–20 mm depth prior to the start of the ponding. (However, for each type of concrete, there was an as measured R_o value for each depth, which was not used to calculate the resistance ratio in order to enable comparison of the relative performance of different types of concrete.) The resistance values obtained just before ponding the specimens with the chloride solution is hereafter referred to as *before ponding* values and those obtained one day after ponding is referred to as *after ponding* values. Separate plots were obtained for the 'before ponding' and 'after ponding' resistance values. Figs. 6–13 report the resistance ratios of the different concrete mixes, both before and after ponding during the weekly chloride ponding cycle. The resistance ratio at duration of ponding equals zero is 1 for the OPC concrete before ponding and the ratio changes for all other cases in relation to this reference value (Fig. 6). Although the resistance was measured between electrodes placed at depths of 10 and 20 mm, 20 and 30 mm, and 30 and 40 mm, the data obtained from the middle set are not included in Figs. 6–13 for clarity.

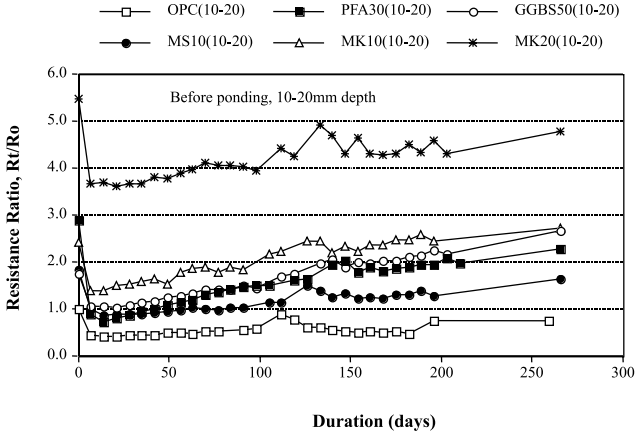

Fig. 6. Resistance ratio of concretes containing OPC and binary blends, 10–20 mm depth values before ponding.

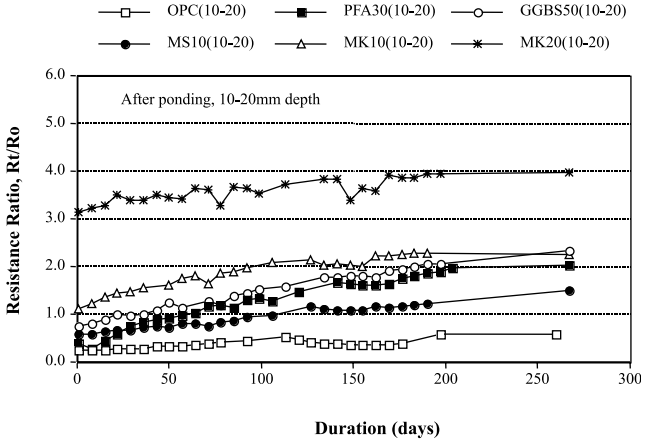

Fig. 7. Resistance ratio of concretes containing OPC and binary blends, 10–20 mm depth values after ponding.

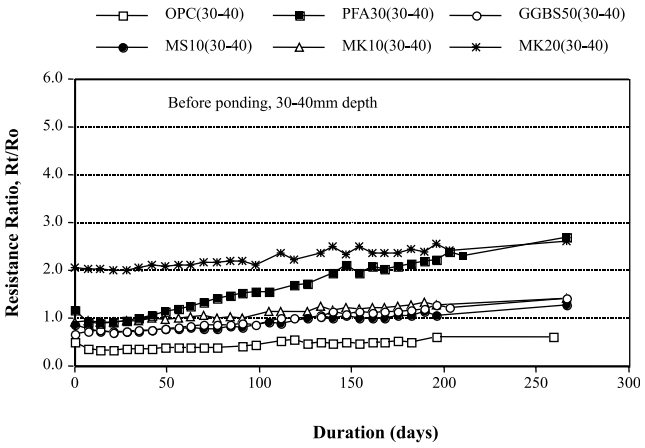

Fig. 8. Resistance ratio of concretes containing OPC and binary blends, 20–40 mm depth values before ponding.

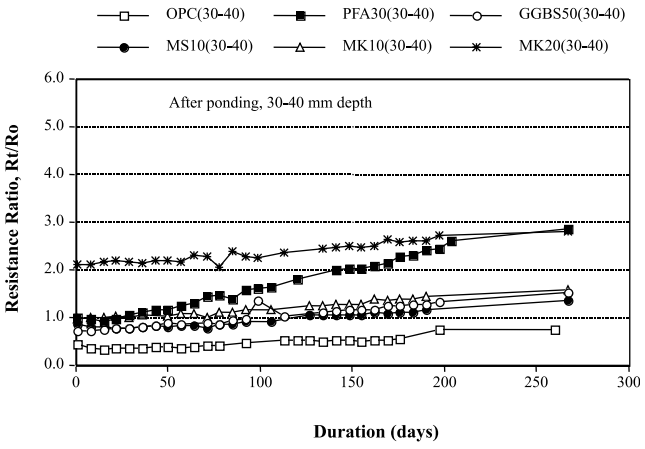

Fig. 9. Resistance ratio of concretes containing OPC and binary blends, 20–40 mm depth values after ponding.

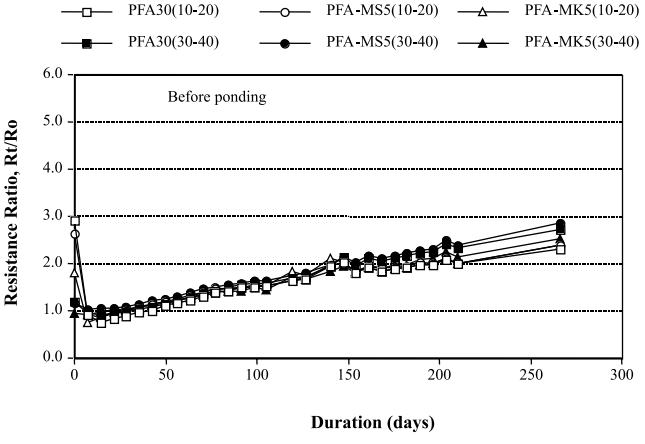

Fig. 10. Resistance ratio of PFA concretes containing ternary blends, before ponding.

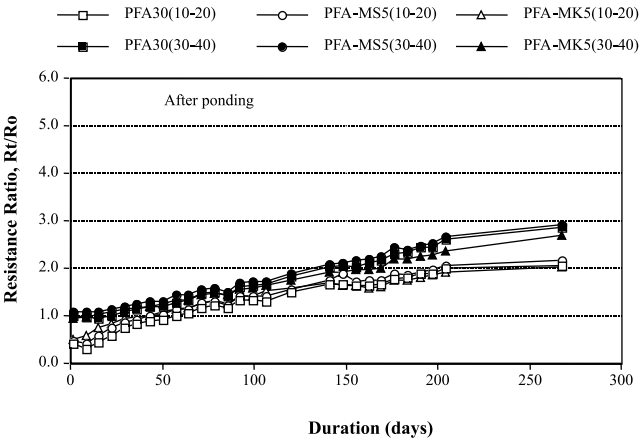

Fig. 11. Resistance ratio of PFA concretes containing ternary blends, after ponding.

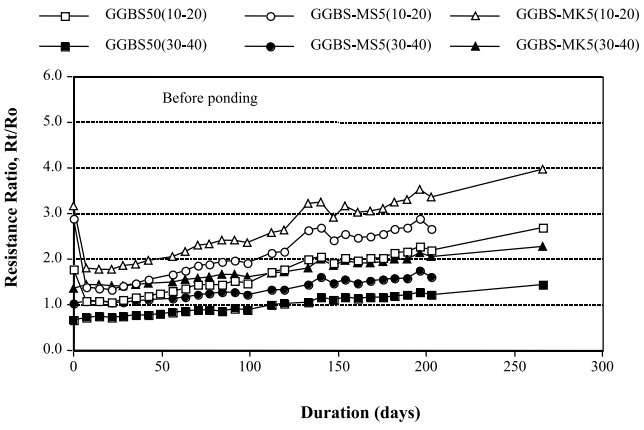

Fig. 12. Resistance ratio of GGBS concretes containing ternary blends, before ponding.

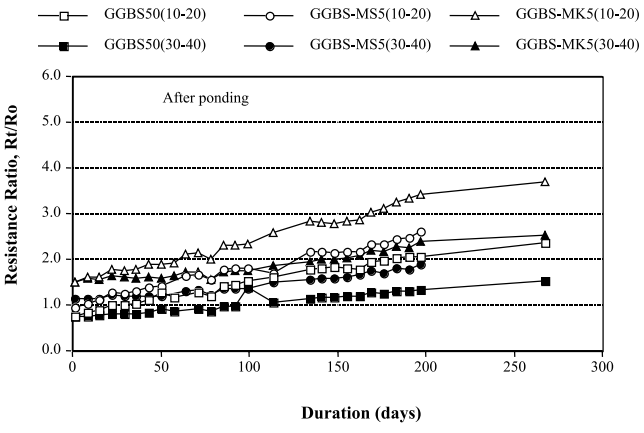

Fig. 13. Resistance ratio of GGBS concretes containing ternary blends, after ponding.

In all these figures, the resistance ratio increased with time, which would mean that the pore structure became less conductive with time. The rate of change of resistance (or conductance) of different concretes due to the cyclic ponding can be obtained by determining the slope of the resistance ratio plots. Similarly, the resistance of the concrete at the start of the test, before there was significant ionic transport in pores, can be obtained by determining the Y-axis intercept of the resistance ratio plots. These two parameters were calculated for all the resistance ratio plots in Figs. 6–13, and are presented in Figs. 14 and 15, respectively. In Fig. 14, in addition to the intercept, the resistance ratios based on the conductance of the dry concrete are also presented, R_o (10–20) BP and R_o (30–40) BP for the two depths. The parameters presented in Figs. 14 and 15 are used to compare the performance of the different types of concrete during the ponding test.

3.2.1. Overall trends

Figs. 6 and 7 present the resistance ratios with exposure time for both the OPC concrete and the concretes containing binary blends, on the basis of measurements carried out between electrodes placed at 10 and 20 mm depths from the surface of ponding. In Fig. 6, the before ponding resistance values were used to calculate the resistance ratios, whereas in Fig. 7 the after ponding values were used. The corresponding resistance ratios on the basis of measurements carried out between electrodes at 30 and 40 mm depths are presented in

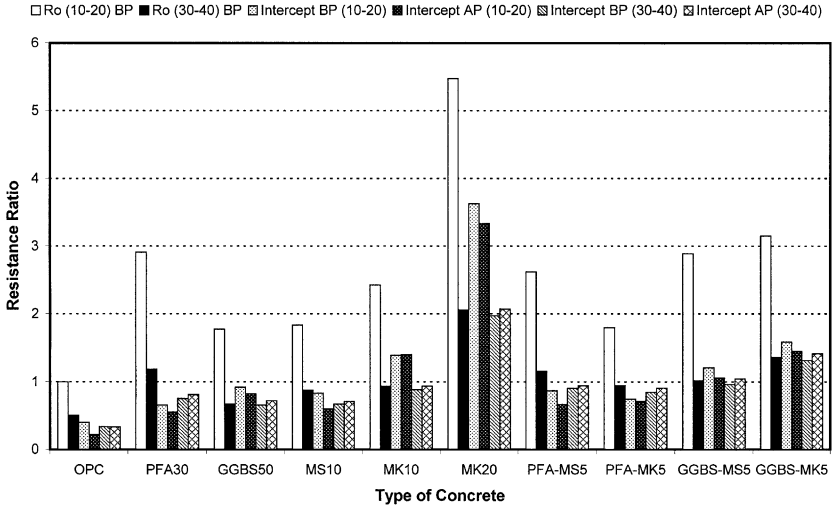

Fig. 14. Initial resistance ratios and resistance ratio intercepts from linear regression analysis.

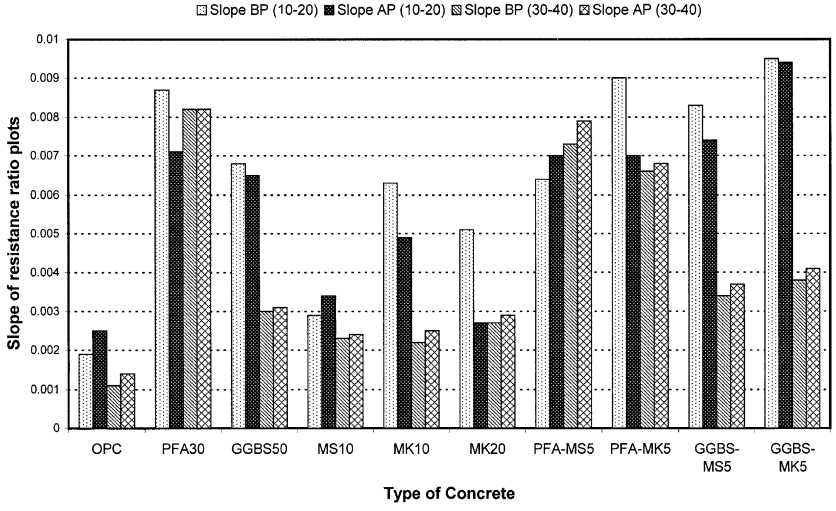

Fig. 15. Rate of change of resistance ratio, from linear regression analysis.

Figs. 8 and 9. The resistance ratios for PFA concretes containing ternary blends are presented in Figs. 10 and 11 for the two cases, viz. before ponding and after ponding. In order to compare their performance with that of the PFA concrete containing the binary blend, the data of the PFA30 were also included in Figs. 10 and 11. Similar comparative data for the GGBS concretes are presented in Figs. 12 and 13.

In Fig. 6 there is a sudden decrease in resistance ratio from the initial value, which then continually improved with time. The concretes were dried prior to the ponding and as a result the pores were relatively empty of moisture at the start of the test. This resulted in relatively high values of resistance. After the first ponding cycle, even though the slabs were exposed to 20 °C and 55% RH for six days, the rate of drying was not adequate to release the moisture from the pores. In addition, chloride ions were absorbed during the first ponding. As a consequence, a lower value of the resistance was measured after the first ponding cycle (Fig. 6). Presumably the moisture state of concrete remained constant thereafter, and the pore structure was modified due to the formation of complex chloro-hydrates when penetrating-chlorides reacted with the hydrates of the cementitious materials. This might have resulted in the increase in resistance with time. Penetrating chlorides could also displace hydroxyl ions due to the ion exchange reaction in the pore solution, which could also increase the resistance of the concretes [17]. The increase in resistance ratios in all cases can be attributed to these changes in the concrete.

The initial decrease in resistance ratio that was observed for the 10–20 mm depth in Fig. 6 was not present for the 30–40 mm data in Fig. 8, except for the PFA30 concrete. The probable reason is that concrete at 30–40 mm depth for these cases was not subjected to any drying even after keeping the specimens at 40 °C and 20% RH for two weeks. In the case of the PFA concretes (for both binary and ternary blends), as can be seen from Fig. 10, there was a sharp decrease in resistance for the 10–20 mm depth values and a small decrease for the 30–40 mm depth values. This would mean the depth of drying was beyond 30 mm in the case of the PFA concretes. The decrease was greater for the 10–20 mm depth data because a greater level of drying was achieved at this depth. The decrease in resistance as a result of the first cycle of ponding for the 10–20 mm depth values and no effect for the 30–40 mm depth values were repeated for the GGBS concretes containing ternary blends in Fig. 12, which confirms that the concrete was not dried out at 30 mm depth from the surface in these cases.

3.2.2. Comparison of resistance ratio curves

The *Y*-axis intercepts of the linear regression lines of the data in Figs. 6–13, after eliminating the initial few data points, are presented in Fig. 14 as Intercept BP (10–20), Intercept AP (10–20), Intercept BP (30–40) and Intercept AP (30–40) for the 10–20 mm depth data before ponding, 10–20 mm depth data after ponding, 30–40 mm depth data before ponding and 30–40 mm depth data after ponding, respectively. The corresponding slopes are presented in Fig. 15 as Slope BP (10–20), Slope AP (10–20), Slope BP (30–40) and Slope AP (30–40). The slopes give the rate of change of the resistance ratio as a result of continued hydration, pozzolanic reaction, chloride binding or a combination of all these effects. The Intercept AP (10–20) and the Intercept AP (30–40) in Fig. 14 represent resistance of the saturated concretes, except that there could be a small error because the values were obtained from the regression analysis of the plots which were influenced by the chloride binding and the degree of pozzolanic activity in the concretes. Nevertheless, when these values are compared with the initial resistance ratios R_o (10–20) and R_o (30–40), respectively, the effect of the saturation can be obtained. The comparisons which can be made from the data in Figs. 14 and 15 are summarised in Table 6, and are discussed below.

Effect of saturation. The effect of saturation was found to lower the resistance between 39% and 81% for the 10–20 mm depth and between 0% and 32% for the 30–40 mm depth. This means that the degree of drying achieved prior to the test was not the same at the two depths; a greater degree of drying was achieved at the 10–20 mm depth. This also depended on the type of concrete. Both the OPC and the PFA30 concretes had the greatest effects at both the depths. The inclusion of both MS and MK in the PFA concrete resulted in a decrease in this effect at both the depths, presumably due to the pore refinement when MS and MK were added. The fact that the resistance ratio increased due to the saturation at the depth of 30–40 mm for the GGBS concretes and MK concretes indicates that there was no moisture movement at this depth during the initial drying. This could be the result of finer pores in these concretes, which require a greater degree of drying to release moisture. However, the result obtained with MS10 was similar to the PFA concretes containing both MS and MK. In summary, the pore structure characteristics of the concretes affected the degree of drying achieved during the initial conditioning of the specimens.

Effect of depth. A negative value in Table 6 under 'effect of depth' means that the 10–20 mm depth performed better than the 30–40 mm depth in relation to both the resistance value at the start and the rate of change of resistance with time. Clearly the effect depended on both the type of concrete and the time at which the resistance measurements were carried out. If the intercepts before ponding are considered first, except in the case of the PFA concretes, the values are negative,

Table 6
Summary of the effects due to cyclic ponding

Mix	Effect of saturation		Effect of depth				Effect of ponding			
	10–20 mm (%)[a]	30–40 mm (%)[b]	Before ponding [c]		After ponding [d]		10–20 mm[e]		30–40 mm[f]	
			Intercept (%)	Slope (%)	Intercept (%)	Slope (%)	Intercept (%)	Slope (%)	Intercept (%)	Slope (%)
OPC	−78	−34	−15	−42	52	−44	−45	32	−2	27
PFA30	−81	−32	15	−6	47	15	−15	−18	8	0
PFA-MS5	−75	−19	4	14	41	13	−23	9	4	8
PFA-MK5	−60	−4	14	−27	28	−3	−4	−22	7	3
GGBS50	−53	7	−29	−56	−13	−52	−10	−4	10	3
GGBS-MS5	−63	2	−20	−59	−1	−50	−13	−11	8	9
GGBS-MK5	−54	4	−17	−60	−3	−56	−8	−1	8	8
MS10	−67	−19	−19	−21	18	−29	−28	17	6	4
MK10	−42	0	−37	−65	−33	−49	1	−22	6	14
MK20	−39	1	−46	−47	−38	7	−8	−47	5	7

[a] Comparison of R_o (10–20) with Intercept AP (10–20).
[b] Comparison of R_o (30–40) with Intercept AP (30–40).
[c] Comparison of both the intercepts and the slopes of BP (10–20) with BP (30–40).
[d] Comparison of both the intercepts and the slopes of AP (10–20) with AP (30–40).
[e] Comparison of both the intercepts and the slopes of BP (10–20) with AP (10–20).
[f] Comparison of both the intercepts and the slopes of BP (30–40) with AP (30–40).

which means that the resistance was greater nearer to the surface for all concretes except the PFA concretes. The increase in resistance at 10–20 mm depth can be attributed to the drying effect when the specimens were stored at 20 °C and 55% RH for six days soon after the ponding for 24 h, despite the penetration of chlorides into this region of the concrete. However, in the case of the PFA concretes, the decrease in resistance could be the effect of unhydrated PFA particles, because they are hydrophilic in nature and could retain a greater amount of water during the storage period. Along with this, the chlorides present might have reduced the resistance at the 10–20 mm depth. The two MK concretes provided the best results.

The change of slope between 10–20 mm depth and 30–40 mm depth before ponding is due to the way the 10–20 mm depth responded to both the chlorides penetrating during ponding and the drying out during the storage at 20 °C and 55% RH for six days. A higher decrease reflects an improvement in resistance with time for the 10–20 mm depth concrete. When this parameter is considered, both the GGBS and the MK concretes were found to be better than the rest and the least performance was obtained with the PFA concretes. As the before ponding resistance is influenced by the drying as well as the penetrating chlorides, results obtained after ponding when the pores are saturated with the chloride solution are more relevant in interpreting the resistance offered by the concretes.

When the concretes were saturated with the chloride solution during the ponding, the near surface resistance values (10–20 mm depth *Y*-axis intercept) were lower than the 30–40 mm depth values for concretes containing OPC, PFA and MS10. However, a reversed trend was obtained for all the GGBS and MK concretes. In both these cases, Figs. 2 and 4 give very low chloride contents and there was very little chloride transport beyond 20 mm depth from the surface. This would support the argument that the mineralogical and the morphological characteristics of these two types of concretes result in a chloride barrier in the very near surface region, which has a beneficial long-term effect in reducing the penetration of chlorides beyond this region. In addition, in the case of the GGBS concretes and MK10, the rate of change of resistance ratio was about 50% higher for the 10–20 mm depth plots. Therefore, the cyclic wetting and drying was found to improve the resistance of the near-surface layer of these two sets of concretes. It is to be noted that the PFA30 and the PFA-MS5 concretes had a decrease in rate of change of resistance with time at 10–20 mm depth compared to 30–40 mm depth. That is, not only the initial resistance was decreased due to the penetration of chlorides, but also the improvement in resistance with time was reduced as a result of the chloride penetration in these cases. This could be due to the lack of binding of chlorides in these two concretes at the near surface region.

Effect of ponding. The effect of ponding here is the change in resistance between before and after ponding for each cycle, as opposed to the continuous effect of the ponding cycles that can be observed from the resistance ratio plots. Therefore, a reduction in intercept indicates

the effect of drying and an increase in slope is due to the combined effects of the drying and the chloride binding. The 10–20 mm depth values indicate that the OPC concrete was most affected by the drying. There has been a consistent decrease in resistance as a result of ponding, except in the case of MK10 concrete, for which the resistance increased modestly. Given the small difference for the MK10 concrete, the results for all concretes can be attributed to the degree of drying for the different concretes. However, when it comes to dealing with the slopes based on the 10–20 mm depth resistance ratio plots, it is to be noted that the slope increased for OPC, PFA-MS5 and MS10 concretes. In all other cases the slope decreased from before ponding to after ponding. As the effect of drying was not separated from the joint effect of continued hydration, chloride binding and the drying due to the storage, no explanation can be provided for this variation.

For the 30–40 mm depth resistance ratios, the intercept was found to increase as a result of ponding in all cases, except the OPC concrete. The probable reason is that only in the case of the OPC concrete, the storage affected the resistance at 30–40 mm depth. There was no significant effect on the rate of change of resistance due to the ponding.

3.2.3. Comparison between different types of concrete

In this section the data in Figs. 14 and 15 are used to compare the performance of the different types of concretes. Fig. 14 shows that the highest initial resistance at the depth of 10–20 mm, denoted by R_o (10–20), was obtained for MK20 concrete, which was approximately 5.5 times that of the OPC concrete. The initial resistance varied between the different types of concretes and the values were in the range 1.8–5.5 times that of the OPC. Both the degree of pozzolanic activity of the ACMs and the degree of drying of various concretes resulted in this variation. As the effect of drying at 30–40 mm depth varied between the different types of concretes, these values are not discussed here, although the values are reported in Fig. 14, as R_o (30–40).

The resistances of the saturated concretes in the cover zone (to be precise in the 10–20 mm depth) are denoted by Intercept AP (10–20) in Fig. 14. It can be seen that the resistance of both the binary blends and the ternary blends was 1.6–9 times higher than that of the OPC. The highest value was obtained for MK20. The influence of both the initial resistance of the dried concrete and the Y-axis intercept of the saturated concrete on the chloride penetration is explored in the next section.

While considering the intercepts before and after ponding at both the depths (Fig. 14), it can be seen that the resistance was the lowest for the OPC concrete and highest for MK20 concrete. For concretes containing binary blends, the resistance was similar for PFA30, GGBS50 and MS10; however, it was greater for both MK10 and MK20. The addition of 5% by mass of MS and MK to the PFA concrete resulted in a modest increase in the values. However, there was a substantial increase for the GGBS concretes, with the addition of MK at 5% by mass resulting in slightly better performance than adding MS at 5% by mass.

Although there were variations between before ponding and after ponding values, the results in Fig. 14 show that these variations are not very high for all the concretes containing ACMs. The same can be said about the depth effect, except for MK10 and MK20 concretes. In these cases, there was a substantial difference between the values at 10–20 mm depth and 30–40 mm depth. As a detailed study of the pore structure characteristic was not carried out in this investigation, no explanation can be provided at present for all the variations observed in the results.

The slopes in Fig. 15 show that the rate of change of resistance with ponding was the lowest for both the OPC and MS10 concretes. The before and after ponding results would suggest that the storage at 20 °C and 55% RH for six days had some effect, but not substantial when compared to the effect of the depth, except in the case of PFA concretes. The reason why the depth effect was very high is because chlorides penetrated up to 20 mm depth in varying quantities even in the case of concretes containing ACMs (Figs. 2–4). This resulted in the pore refinement due to chloride binding and/or the formation of chloro-aluminates at the top layer, which did not occur at the deeper layer. The change in slope of the PFA concretes might have been the result of its increased pozzolanic activity at both the depths. While considering the change in slope, i.e., the improvement in resistance with time, as a performance indicator, the best performance was observed for the three GGBS concretes.

3.3. Relationships between resistance measurements and chloride penetration

In an attempt to explore the possibility of relating data from embedded resistance probes to the chloride penetration in concretes containing ACMs, the initial resistance ratios R_o (10–20) BP and R_o (30–40) AP from Fig. 14 are plotted against the apparent diffusion coefficient calculated from the chloride profiles, in Fig. 16. Although a general trend can be observed, the degree of dependence was not very high. The after ponding results, of the saturated concretes, were found to have a better correlation with the apparent diffusion coefficient. It must be remembered that the resistances were measured along the depth rather than parallel to the exposure surface in this investigation. Had the measurements

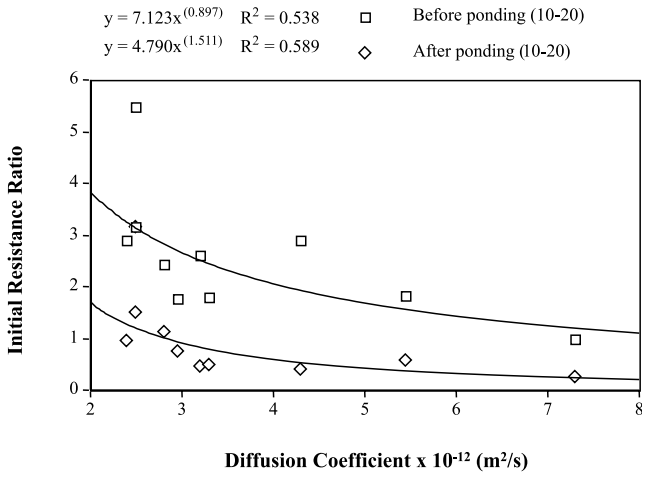

Fig. 16. Relationship between initial resistance ratio and apparent diffusion coefficient.

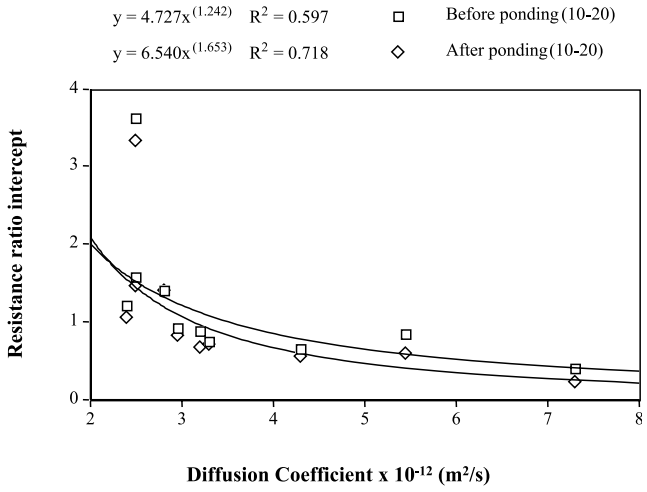

Fig. 17. Relationship between resistance ratio intercept and apparent diffusion coefficient.

been carried out parallel to the surface, the correlations would have been better.

In Fig. 17, the resistance ratio intercepts from the 10–20 mm depth data are plotted against the apparent diffusion coefficient. As the resistance ratio intercepts reflect also the continued change in resistance due to the penetration of chlorides, a better correlation was found in Fig. 17, especially for the saturated samples. The two data points lying away from the trend line represent the high resistance values of the MK concretes. Both Figs. 16 and 17 suggest that the resistance measurements of the saturated concretes containing ACMs can be used to determine the chloride ion penetration resistance of these concretes. However, further research where the electrodes are embedded parallel to the surface would be

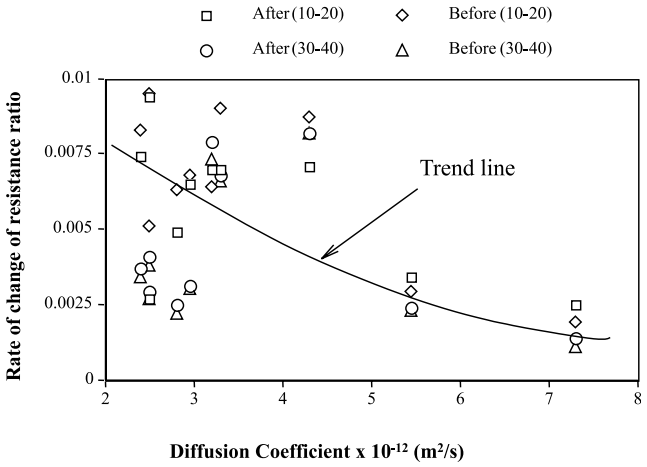

Fig. 18. Relationship between rate of change of resistance ratio and apparent diffusion coefficient.

desirable so that a more reliable relationship between the resistance ratio and the apparent chloride diffusion coefficient could be developed.

Finally, the relationship between the rate of change of resistance ratio with time and the apparent diffusion coefficient is presented in Fig. 18. The degree of dependence was not determined in this case because of the large scatter of data at the lower end of the diffusion coefficient. However, the trend line shows that the resistance change with time could also be useful in determining the chloride ion penetration resistance of concretes containing ACMs.

4. Conclusions

On the basis of an investigation of chloride penetration and resistance change with time of concretes containing ACMs, the following conclusions have been drawn:

(i) After subjecting both the OPC and ACM concretes to a cyclic chloride ponding regime for a year, it was observed that the chloride penetration beyond 30 mm was very small for concretes containing ACMs. However, there was substantial penetration of chlorides beyond this depth for the OPC concrete. The concretes containing binary blends of OPC with PFA, GGBS, MS and MK provided resistance to the chloride penetration in varying degrees. The best performance was found to be with GGBS and MK, both of which largely prevented the penetration of chlorides beyond 20 mm. Both the PFA and MS concretes did not perform as well as the GGBS and MK concretes. When these materials were used as a ternary blend, PFA along with both MS and MK provided an improvement, however, there was a small detrimental effect for the GGBS concrete when

GGBS was used in ternary blended form along with both MS and MK.

(ii) The arrival of a chloride-laden solution at the level of electrodes embedded in concretes was found to reduce the resistance substantially and the degree of reduction depended on the type of the concrete. Both the degree of drying prior to the ponding and the amount of chloride-laden solution arriving at the first line of embedded electrodes were found to be highest for both the OPC and PFA concretes. The best results were obtained with MK20 and GGBS50 concretes. There was some beneficial effect due to the addition of both MS and MK at 5% by mass to the PFA concrete.

(iii) The resistance of the concrete was found to increase with time during the ponding period and this also depended on the type of the concrete. The change in resistance was higher for the top layer of concrete than the deeper layers. This is considered to be due to the pore refinement as a result of either chloride binding or the formation of chloro-aluminates, or the combination of both these. The best performance was obtained for GGBS and MK20 concretes. The resistance change in OPC, PFA and MS10 concretes were relatively small, presumably because there was not much chloride binding for these concretes at the top layer.

(iv) It was found that the resistance measurements and parameters obtained from the change in resistance with time for concretes containing ACMs could be related to their chloride diffusion characteristic. However, this research needs to be repeated with the arrangement of electrodes parallel to the exposure surface so that better correlations between the two could be obtained.

Overall the placement of electrodes provided much useful information, which could not have been obtained with other conventional methods of investigation.

Acknowledgements

The authors acknowledge the European Social Fund for providing support to carry out this research. The facilities provided by the School of Civil Engineering are also acknowledged.

References

[1] Jones AEK et al. Development of an holistic approach to ensure the durability of new concrete construction. Report for the Department of Environment, Project 38/13/21 (cc1031), British Cement Association, October 1997, 78 pp (ISBN 0-7210-1522-0).
[2] Mc Carter WJ, Emerson M, Ezirim H. Properties of concrete in the cover zone: developments in monitoring techniques. Mag Concr Res 1995;47(172):243–51.
[3] Li S, Roy DM. Investigation of relations between porosity, pore structure and chloride diffusion of fly ash and blended cement pastes. Cem Concr Res 1986;16:749–59.
[4] Mehta PK. Pozzolanic and cementitious by-products as mineral admixtures for concrete: a critical review. Am Concr Inst 1983; SP-79:1–46.
[5] British Standards Institution, BS882: Specification for aggregates for concrete, BSI, London, 1982.
[6] British Standards Institution, BS1881: Part 125: Methods for mixing and sampling fresh concrete in the laboratory, BSI, London, 1986.
[7] British Standards Institution, BS1881: Part 102: Method for determination of slump, BSI, London, 1983.
[8] British Standards Institution, BS1881: Part 103: Method for determination of compacting factor, BSI, London, 1982.
[9] Basheer PAM, Nolan E, Mc Carter WJ, Long AE. Effectiveness of in-situ preconditioning methods for concrete. ASCE J Mater Civil Eng 2000;12(12):131–8.
[10] Whittington HW, Mc Carter WH, Forde MC. The conduction of electricity through concrete. Mag Concr Res 1981;33(114):48–60.
[11] Longuet P. La protection des armatures dans le béton armé élaboré avec des ciments de laitier, Nos. 7/8, 1976, p. 321–328.
[12] Buenfeld NR, Newman JB, The resistivity of mortars immersed in sea-water. Cem Concr Res 1986;16(4):511–524.
[13] Buenfeld NR, Newman JB. Examination of three methods for studying ion diffusion in cement pastes, mortars and concretes. Mater Struct 1987;20:3–10.
[14] Christensen BJ, Mason TO, Jennings HM. Influence of silica fume on the early hydration of Portland cements using impedance spectroscopy. J Am Ceram Soc 1992;75(4):939–45.
[15] Christensen BJ et al. Impedance spectroscopy of hydrating cement-based materials: measurement, interpretation, and applications. J Am Ceram Soc 1994;77(11):2789–804.
[16] Poulsen E. The chloride diffusion characteristics of concrete, approximate determination by linear regression analysis. Nordic Concrete Research, Publication No. 9, Nordic Concrete Federation, 1990.
[17] Chatterji S. Transportation of ions through cement based materials, Part 3: Experimental evidence for the basic equations and some important deductions. Cem Concr Res 1994;24(7):1229–36.
[18] Teychenne DC, Franklin RE, Erntroy HC. Design of normal concrete mixes. Department of the Environment, London, H.M.S.O., 1975, 30 pp.